

THE INTERACTION OF SOFC ANODE MATERIALS WITH CARBON MONOXIDE

REAKCIJE MED ANODNIMI MATERIALI SOFC IN OGLJIKOVIM MONOKSIDOM

Barbara Novosel¹, Mihael Avsec², Jadran Maček¹

¹Faculty of Chemistry and Chemical Technology, University of Ljubljana, Aškerčeva 5, 1000 Ljubljana, Slovenia

²CHEMASS, Babičeva ul. 1, 1000 Ljubljana, Slovenia
barbara.novosel@fkkt.uni-lj.si

Prejem rokopisa – received: 2007-10-08; sprejem za objavo – accepted for publication: 2008-01-23

High-temperature solid-oxide fuel cells (SOFCs) are modern systems used for the transformation of chemical energy into electrical energy. The main problem in their development is related to the materials used for their construction, e.g., electrodes, electrolytes, interconnects, etc. The ageing of the electrocatalysts, the anode and the cathode, produces microstructural changes due to the high operating temperature, and in the case of the internal steam reforming of the fuel, due to the interaction of the anode material in contact with the gaseous phase. In the latter case, deactivation of the anode is caused by the deposition of carbon, which hinders the fuel transport on, and in, the porous anode. This carbon deposition is the consequence of the methane dehydrogenation reaction or Boudouard's equilibrium reaction. The reaction of carbon monoxide with the anode material is the focus of the present study.

A composite anode material made of nickel and yttria-stabilized zirconia was exposed in a micro-reactor, at different temperatures, to a gas mixture of carbon monoxide (4 %) and argon (96 %). Depending on the cermet sample and the conditions in the micro-reactor, Boudouard's equilibrium was established, accompanied by the formation of carbon deposits. The amount of carbon deposited and its reactivity was determined later by a temperature-programmed oxidation in air. The interval of the oxidation temperature for carbon isothermally deposited at temperatures of 400 °C, 500 °C, 600 °C and 700 °C was found to lie in the temperature range from 476 °C to 610 °C. Less-reactive forms of carbon were obtained by depositing at higher temperatures. The changes in the composition of the gas phase in contact with the anode material were followed by on-line coupled mass spectrometry and gas chromatography.

Key words: carbon deposition, carbon monoxide, Boudouard's equilibrium, SOFC

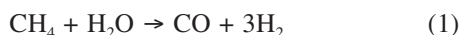
Visokotemperaturne gorivne celice SOFC so sodobni sistemi za pretvorbo kemične v električno energijo. Glavni problem pri njihovem razvoju so konstrukcijski materiali, kot so elektrode, elektrolit, vmesnik idr. S staranjem elektrokatalizatorjev, anode in katode nastajajo mikrostrukturne spremembe zaradi visoke delovne temperature in interakcije anodnega materiala s plinsko fazo v primeru parnega reforminga goriva. Sčasoma se pojavi deaktivacija anode, zaradi nanosa ogljika, ki ovira transport goriva na in v pore anode. Nanesen ogljik je posledica reakcije dehidrogenacije metana ali reakcije Boudouardovega ravnotežja. Reakcija ogljikovega monoksida z anodnim materialom je predmet predloženega dela.

Kompozitni anodni material niklja in stabiliziranega itrijevega oksida je bil v mikroreaktorju izpostavljen plinski zmesi ogljikovega monoksida (4 %) in argona (96 %) pri različnih temperaturah. V odvisnosti od kermetnega materiala in razmer v mikroreaktorju se je vzpostavilo Boudouardjevo ravnotežje s sočasnim nanosom ogljika. Količina nanesenega ogljika in njegova reaktivnost je bila določena kasneje s temperaturno programirano oksidacijo v zraku. Temperaturni interval oksidacije ogljika, ki je bil nanesen v izotermnih razmerah pri 400 °C, 500 °C, 600 °C in 700 °C, je v temperaturnem območju med 476 °C in 610 °C. Manj reaktivne oblike ogljika so nastajale pri nanosu pri višji temperaturi. Spremembe sestave plinske faze pri kontaktu z anodnim materialom smo spremljali z masno spektrometrijo in plinsko kromatografijo.

Ključne besede: nanos ogljika, ogljikov monoksid, Boudouardovo ravnotežje, SOFC

1 INTRODUCTION

The main advantage of SOFCs with respect to other types of energy converters is the possibility of using methane and other hydrocarbons, even biogas derived from biomass gasification, as fuels ¹. This is enabled by conducting internal steam reforming and water gas shift reactions in the anode layer of the SOFC membranes:



Some undesired side reactions can occur that lead to carbon deposition on, and in, the porous anode ²:



The material deposited according to reaction (3) is usually called coke, and that deposited by reaction (4), carbon ³. In coke, besides carbon, also some heavier polymeric hydrocarbon chains are found ⁴. The problems associated with carbon deposition were known from the beginning of the research on SOFCs, and even before that the petrochemical industry had similar problems with steam-reforming processes. In these processes methane (or a heavier hydrocarbon) is reacted with steam in a molar ratio of at least 2:1 (H₂O:CH₄). In the presence of a nickel catalyst at temperatures of 800 °C or above, a synthesis gas consisting of a mixture of hydrogen and carbon monoxide is produced. During the prolonged operation of the steam reformer, carbon deposits occur but in a petrochemical plant they are easily dealt with by flushing the catalyst with steam and

thus converting the deposits to carbon monoxide and hydrogen. In the case of fuel cells the anode material consists in most cases of a nickel cermet, the ceramic matrix being yttria-stabilized zirconia. Regeneration by steam flushing is not appropriate since it can lead to the reoxidation of the nickel to nickel oxide and an associated volume expansion of the nickel phase that can impair the anode layer. The greater sensitivity of the anode layer to the harmful effect of steam flushing results from dimensional and functional factors. The thickness of the anode layer ranges from several tens of micrometers to several hundred micrometers in the case of an anode-supported cell, as compared to catalyst particles for industrial steam reforming that are in the range of centimetres. Any volume expansion in the anode layer can lead to cracking and delamination from the electrolyte layer. Even minor changes in the micro-morphology of the anode can also lower its conductivity.

Carbon deposition problems for SOFCs running on hydrocarbons are usually dealt with by an appropriate steam-to-carbon ratio of more than 2 : 1. For the commercial use of SOFCs the expected lifetime of a cell is very important. Besides solving problems associated with the ageing and poisoning of the cell's electro-catalysts, the prevention of coking is of utmost importance and can markedly enhance the lifetime of the cell, which should be 40,000 h or more ⁵.

2 EXPERIMENTAL

The samples of anode material, i.e., a composite of nickel and yttria-stabilized zirconia (Ni/YSZ), were of commercial origin. The sample designated as FCM was a nickel oxide and yttria-stabilized zirconia powder (with mass fractions 66 % NiO and 34 % YSZ-8 (mole fraction 8 % Y₂O₃), with a surface area of 5.65 m²/g) from Fuel Cell Materials, OH, USA. Sample IAM was obtained from Inframat® Advanced Materials, USA, Nanox 28ZY8-1 (sample volume fractions of composition Ni/YSZ 50/50 %, surface area 66.87 m²/g). For baseline measurements Tosoh – Zirconia TZ-8Y yttria-stabilized zirconia powder, from the Tosoh Corporation, Japan was used.

The gases were simultaneously analysed by an Inficon Quadrex 200 mass spectrometer (input pressure 1 mbar, head pressure $3.3 \cdot 10^{-6}$ mbar, or $6.6 \cdot 10^{-6}$ mbar, gain $6 \cdot 10^{-11}$ A, scan time 2.703 s, scanning borders 0-50 amu) and Agilent Micro GC 3000A gas chromatograph (carrier gas argon 5.0, analytical columns: Plot U, Plot Q with timed controlled injector and molecular sieve with backflush input, detector type: TCD, inlet temperature 140 °C, injector temperature 100 °C, column temperature 100 °C for Plot U, 70 °C for Plot Q and 80 °C for molecular sieve, column pressure 2.068 bar for Plot U and Plot Q, 2.206 bar for molecular sieve, analysis run

time 180 s). The testing system set-up has been described elsewhere ⁶.

The amount of deposited carbon was determined by temperature-programmed oxidation of a known amount (1.5 mg) of carbon (soot Printex) in the testing system. By determining the area under the carbon dioxide curve obtained by integration, the correlation factor was obtained and used for quantification of the MS and GC results.

3 RESULTS AND DISCUSSION

The deposition of carbon on the SOFC anode can be attributed to three main reactions (3-5) and depends on the conditions in the cell, e.g., the steam-to-fuel ratio, the temperature, the flow rate etc., as well as on the anode material and its characteristics (composition and micro-morphology). More research has been done on coke deposition from hydrocarbon fuels (3) and less on carbon deposition from the carbon monoxide disproportionation reaction (4). The well-known Boudouard's equilibrium implies that at higher temperatures carbon monoxide will be stable and that at lower temperatures the deposition of carbon can be expected. A general trend in SOFC development is lowering of the operating temperature of the cell, which ten years ago was approximately 1000 °C. Nowadays the operating temperatures have dropped to 750 °C and even lower values have been mentioned in the literature ^{7,8}. This is within the temperature region where carbon deposition is expected and this research work was directed towards studying this phenomenon.

The carbon deposition was tested with contacting samples of anode material in powdered form with a mixture of the volume fraction of carbon monoxide (4 %) and argon (96 %) under temperature-programmed and isothermal conditions. The anode materials were characterized with electron microscopy and specific-surface-area measurements. The FCM material is a fine powder with an average particle size below one micrometer. The IAM material differs appreciably in particle size, which is several ten micrometers of the agglomerates of smaller particles. The specific-surface-area measurements show a roughly tenfold difference between the two samples. Although it could be expected that the finer material would have a larger specific area, this was not the case, the FCM sample had 5.65 m²/g and the IAM sample, 66.87 m²/g, which can be attributed to the porosity of the agglomerated particles in this sample.

The carbon deposition was followed by a system for determining the interaction of solid materials with the gaseous phase ⁶. The system consisted of a gas-supply system, a furnace with a quartz micro-reactor and a temperature controller, a quadrupole mass spectrometer, gas chromatograph and PC where all the data are collected and stored. In the case of studies of the dehydrogenation of methane, the evolution of hydrogen was monitored as a measure of carbon deposition, while

for the carbon monoxide disproportionation reaction carbon dioxide was determined. Gas-analysis methods were chosen because of their sensitivity compared to thermogravimetry and other analytical techniques.

The testing protocol began with the temperature-programmed reduction (TPR) of the sample in an argon/hydrogen mixture for converting nickel oxide to metallic nickel, followed by cooling of the furnace to room temperature in the same atmosphere. The second phase was either the temperature programmed (TPD) or the isothermal deposition (ITD) of carbon from the argon/carbon monoxide mixture. The third step, after cooling the sample to room temperature, was the temperature-programmed oxidation (TPO). This set of experiments was carried out on the anode materials to find which one was less susceptible to carbon deposition. Therefore, the conditions for higher rates of carbon deposition, achieved by omitting the addition of steam into the gas stream, were created intentionally.

The carbon deposition on a fuel cell occurs mainly due to reactions (3) and (4). For comparison TPD was also carried out from a mixture of methane with argon, leading to coking of the electrocatalyst⁹. In this case carbon deposition follows the reaction path (3) and the hydrogen concentration in the carrier gas is a measure of the carbon deposited (**Figure 1**).

This figure shows that on the FCM sample no carbon was deposited until a temperature of 439 °C was reached, when the heterogeneous thermal dissociation of methane according to reaction (3) started. At 527 °C the maximum concentration of hydrogen was observed. With a further increase in the temperature, the hydrogen

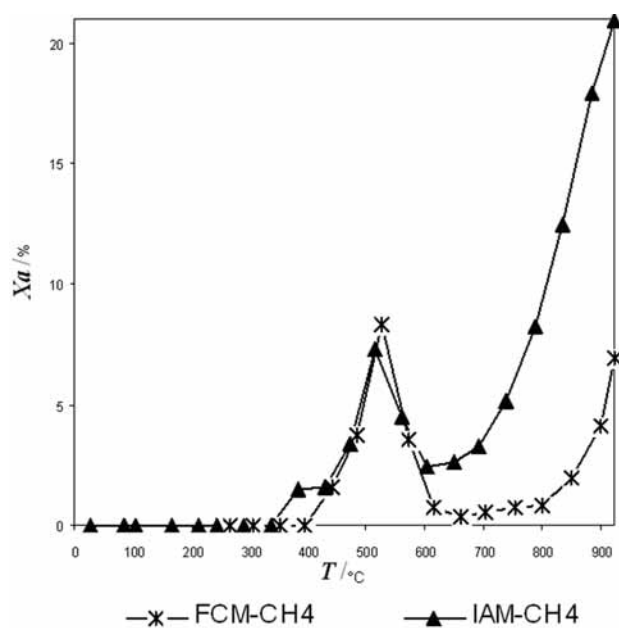


Figure 1: Deposition from methane, degree of conversion of CH₄ vs. temperature

Slika 1: Nanos iz metana; stopnja konverzije CH₄ v odvisnosti od temperature

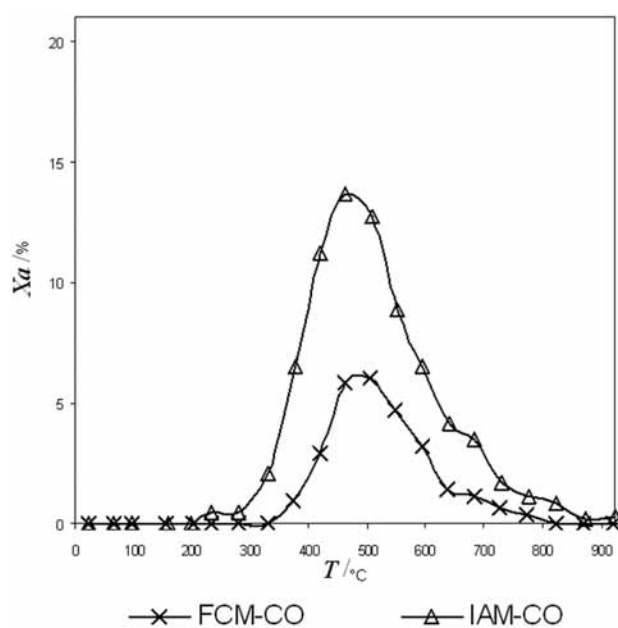


Figure 2: Deposition from carbon monoxide, degree of conversion of CO vs. Temperature

Slika 2: Nanos iz ogljikovega monoksida; stopnja konverzije CO v odvisnosti od temperature

concentration decreased and reached a minimum at 661 °C. Up to 800 °C the hydrogen concentration stayed almost at the same low level and above this temperature it rose more steeply again. The IAM sample behaved similarly but with a small preceding peak before the larger one at 337 °C. In this case also the hydrogen concentration above this temperature decreased again, but it never reached such low values as in the case of FCM and it started to rise much more steeply after 694 °C. We assume that for the first peak coverage of the active sites on the nickel particles occurred. With increasing temperature the carbon starts to deposit over the whole material and onto already deposited carbon, accompanied by an intensive evolution of hydrogen.

The deposition of carbon from the disproportionation reaction of carbon monoxide (4) was carried out initially with the aim to obtain an overview of the system using a dynamic test with temperature-programmed heating of both samples up to 930 °C in an argon/carbon monoxide mixture. The deposition of carbon was followed by measuring the concentration of carbon dioxide in the carrier gas according to reaction (4). For sample FCM the evolution of carbon dioxide started at 374 °C and reached a maximum concentration at 505 °C (**Figure 2**). The rate of CO₂ evolution changed again at 637 °C and decreased practically to zero at 822 °C. In the case of the IAM sample the first evolution of carbon dioxide occurred at 232 °C. A small peak preceded a much larger one. The highest carbon dioxide concentration was obtained at 464 °C. With increasing temperature the carbon dioxide concentration diminished with two distinctive shoulders at 639 °C and 730 °C. The

maximum conversion of carbon monoxide into dioxide was twice that of the IAM sample.

Isothermal deposition tests (ITD) were made at temperatures of 400 °C, 500 °C, 600 °C and 700 °C. The samples were first heated in an argon atmosphere. After the pre-selected temperature was reached, the furnace was set to the isothermal mode and the atmosphere was exchanged for a mixture of carbon monoxide and argon. After 80 minutes of deposition the atmosphere was again changed to argon and the furnace cooled down to room temperature. The result the ITD sample gave was the curves for carbon dioxide concentration in the carrier gas vs. time. The general shapes of the curves for both samples are similar, with significant differences in the peak concentration and the decay line. The carbon dioxide concentration first steeply increased and in approximately 5 min reached its maximum. The peak height for the FCM sample was the highest for carbon deposited at 500 °C followed by 400 °C, 700 °C and 600 °C (Figure 3). With increasing temperature the concentration falls off, but at different rates. For all the samples the curves almost level off after 80 min. Although the concentration of carbon dioxide levels off it does not return to zero even after 80 min. The concentration of carbon dioxide remaining in the carrier gas is very similar for three temperatures but more than twice as high for the sample prepared at 600 °C. The IAM anode material shows a similar behaviour (Figure 4). The peak carbon dioxide concentrations follow the same order as for the FCM sample, but appreciably different decay curves were observed. The sample obtained at 600 °C levels off first, followed by the one prepared at 700 °C. The residual concentration of carbon dioxide is more than three times as high for the sample prepared at 600

°C than for the one prepared at 100 °C higher. The samples prepared at 500 °C and 400 °C do not reach the level of constant CO₂ concentration. In all four cases the deposition proceeds even after 80 min.

The ITD follows the expected pathway. When carbon monoxide comes into contact with fresh anode material, the deposition abruptly starts to produce a very sharp peak.

Samples with deposited carbon prepared during the isothermal deposition tests were left in quartz micro-reactors to cool down. After the atmosphere was changed to dry air, they were reheated in the temperature-programmed mode to 800 °C.

The TPO of the samples provides us with several data, e.g., the initial temperature of the carbon oxidation, the temperature interval in which it is oxidized and the amount of carbon deposited. During TPO carbon is oxidized to dioxide and transferred by the carrier gas to GC and MS. The results of the temperature-programmed oxidation for both samples are presented in Figures 5 and 6. Carbon was deposited from 400 °C to 700 °C in 100 °C increments. The TPOs of the FCM reveal three different curves for the deposited carbon. That obtained at 400 °C oxidizes at 517 °C producing a small peak (compared to the others). Carbon deposited at 500 °C and 600 °C oxidizes at 520 °C and 555 °C, respectively, producing sharp and narrow peaks. Carbon deposited at 700 °C produces a very broad peak extending over a wide temperature interval. The amount of carbon dioxide released was appreciably lower than in the other cases, so the results for this curve were obtained by GC instead of by MS which was used in the other three instances.

A comparison was made of the FCM results and those obtained for the second material. The IAM shows a

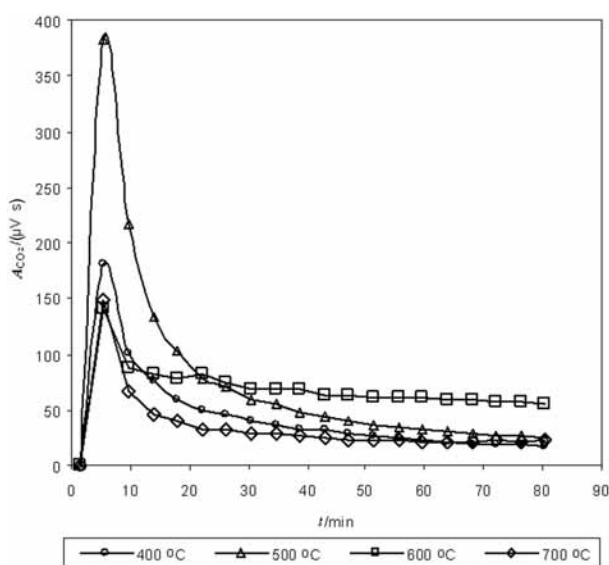


Figure 3: TPD of FCM sample at different temperatures, $A_{CO_2}/(\mu V s)$ GC signal

Slika 3: TPD vzorca FCM pri različnih temperaturah, $A_{CO_2}/(\mu V s)$ za GC signal

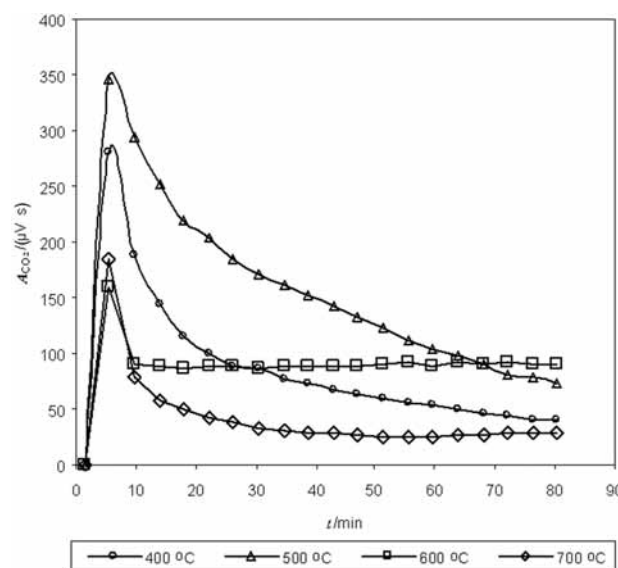


Figure 4: TPD of IAM sample at different temperatures, $A_{CO_2}/(\mu V s)$ GC signal

Slika 4: TPD vzorca IAM pri različnih temperaturah, $A_{CO_2}/(\mu V s)$ za GC signal

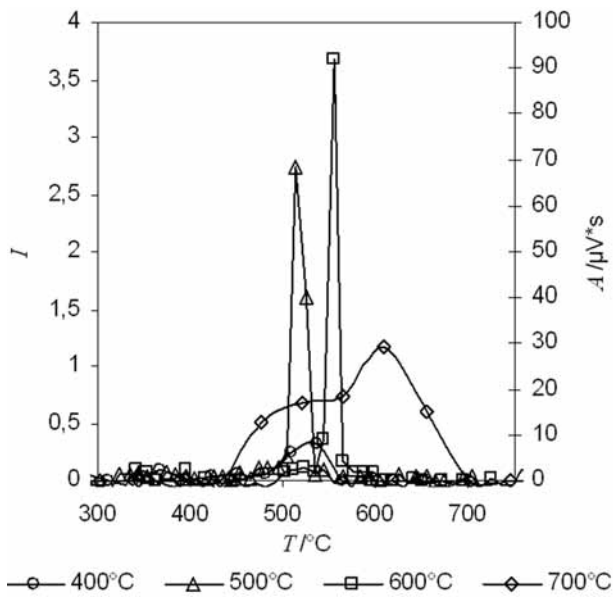


Figure 5: CO₂ evolution during TPO of carbon previously deposited at 700 °C on FCM sample/*I* – intensity of MS signal, *A*/(μV s) GC signal

Figure 5: Sproščanje CO₂ med TPO ogljika predhodno deponiranega pri 700 °C na vzorcu FCM/*I* – intenziteta za MS signal, *A*/(μV s) za GC signal

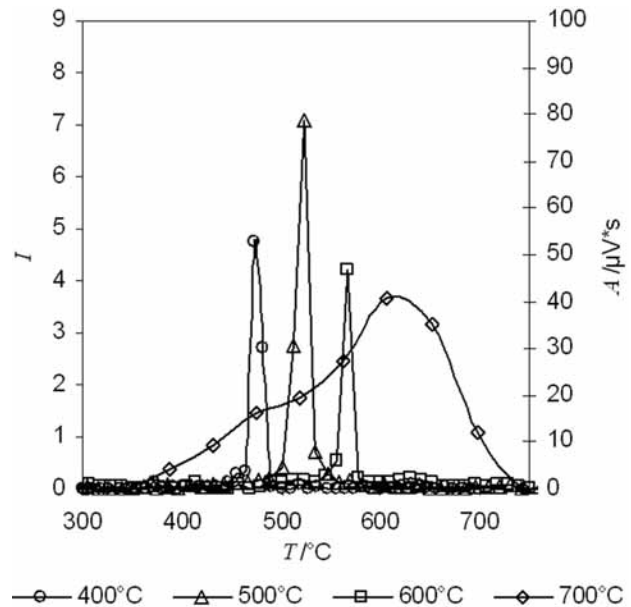


Figure 6: CO₂ evolution during of carbon previously deposited at 700 °C on IAM sample/*I* – intensity of MS signal, *A*/(μV s) GC signal

Figure 6: Sproščanje CO₂ med TPO ogljika predhodno deponiranega pri 700 °C na vzorcu IAM/*I* – intenziteta za MS signal, *A*/(μV s) za GC signal

similar outcome (**Figure 6**). The greatest difference between the two sets of data is in the initial temperature and the height of the peak for deposition at 400 °C. For the IAM sample this peak is large and sharp with a peak temperature of 476 °C. The positions of the peaks for the samples obtained at 500 °C and 600 °C do not change significantly on the temperature scale. The peak for the IAM sample deposited at 700 °C again differs appreciably from the other three, although the shape is similar to the one obtained at the same temperature for the FCM sample. It also shows a bimodal shape but extends across

an even wider temperature interval, from 342 °C to 742 °C.

A comparison of the masses of carbon deposited per mg of sample shows that at all four temperatures the amount of deposited carbon is from 1.7 to 3.5 times higher in the case of the IAM sample (**Table 1**). The greatest discrepancy is at the lowest temperature of deposition. This is in accordance with the specific-surface-area measurements, where the IAM sample has around a tenfold larger specific area than the FCM sample.

Table 1: Amount of deposited carbon

Tabela 1: Količina nanesenega ogljika

<i>T</i> _{deposition} (°C)	FCM sample			IAM sample			IAM:FCM (10 ⁻²)
	<i>m</i> _{Ni-YSZ} (mg)	<i>m</i> _C (mg)	<i>m</i> _C / <i>m</i> _{Ni-YSZ} (10 ⁻³)	<i>m</i> _{Ni-YSZ} (mg)	<i>m</i> _C (mg)	<i>m</i> _C / <i>m</i> _{Ni-YSZ} (10 ⁻³)	
400	41.82	0.228	5.4	43.28	0.832	19.2	3.5
500	41.93	0.619	14.8	42.18	1.818	43.1	2.9
600	43.19	0.576	13.3	42.40	0.938	22.1	1.6
700	41.70	0.098	2.3	42.24	0.173	4.1	1.8

Table 2: Temperature of oxidation of carbon deposits

Tabela 2: Temperatura oksidacije nanesenega ogljika

<i>T</i> _{deposition} (°C)	FCM sample				IAM sample			
	<i>T</i> _{initial} (°C)	<i>T</i> _{peak} (°C)	<i>T</i> _{end} (°C)	<i>T</i> _{end} - <i>T</i> _{initial} (°C)	<i>T</i> _{initial} (°C)	<i>T</i> _{peak} (°C)	<i>T</i> _{end} (°C)	<i>T</i> _{end} - <i>T</i> _{initial} (°C)
400	475	517	567	92	436	476	493	57
500	445	520	550	105	465	520	587	122
600	491	555	606	115	479	569	650	171
700	432	609	700	268	342	652	742	320

The TPO results show more than just the amount of deposited carbon, and from these data, and especially its oxidation temperature, conclusions about the reactivity of the deposit may be drawn (**Table 2**). With other parameters being the same or at least similar, the oxidation temperature of the carbon deposited on the sample mainly depends on the allotropic form of the carbon, the particle size, the shape and the porosity. Graphite is less reactive towards oxidation than soot⁶. A higher reactivity of carbon is advantageous since it increases the possibility that it will react with water vapour.

It is known that carbon species deposited at lower temperatures exhibit a higher reactivity than those deposited at higher temperatures¹⁰. From our data it can be concluded that at 700 °C the mechanism and the product of this deposition reaction are significantly different from those obtained at 600 °C. For the FCM sample 6.1 times less carbon is deposited at 700 °C than at the previous temperature of 600 °C, and for the IAM sample the value is 5.4 times less. The very broad peak of the bimodal shape could also indicate that several carbon species with different reactivities are deposited.

The above-mentioned trend for lowering the operating temperatures of SOFCs will simplify the choice of materials for them and reduce some constructional problems, but it may also enhance the carbon deposition rate and the associated problems. The carbon deposition from carbon monoxide disproportionation may occur not only during the operation but also during the startup and shutdown of the cells when the system passes through temperature regions where carbon deposition is favoured.

The catalytic effect of the anode material on the fuel has already been studied, but in SOFCs running on the internal reforming mode it is also important to know its effect on the Boudouard equilibrium reaction. By determining the reactivity of carbon from different sources, i.e., reactions, it is possible to predict which form has the most detrimental effect on the operation of the cell. Even if the contribution to the deposition of carbon from Boudouard's reaction is not dominant in terms of mass, the early formation of stable nuclei can speed up the deposition by hydrocarbon dehydrogenation.

Complex equilibria are established between the gases in the porous anode material, with some of the reactions leading to carbon deposition. In spite of the strong interrelationship between the reactions occurring in the anode, they can nevertheless be studied individually and the contribution of each to the whole system determined. It is important to know which reaction contributes most to the formation of deposits, what is the nature of the deposit and if a suitable change in the composition and the micro-morphology can diminish it.

The conditions used for the tests presented in this study are not the same as those in the anode during its

operation. It is desirable that all nickel particles are connected with adjacent nickel particles and similarly also all YSZ particles are part of an interconnected 3D network, which enables the transfer of oxygen ions in the depth of the anode. The main difference between our conditions and those in the fuel cell is the absence of a flow of oxygen ions into the anode and the electron transfer out of it. The conditions at a particular micro-location can, however, be similar to ours because all of the particles of both phases are not a part of such a continuum. The presence of water vapour was intentionally omitted to speed up the deposition rate and shorten the duration of the experiments. In order to carry out the tests under more realistic conditions, it should be introduced into the system and thus the results under dry conditions verified.

4 CONCLUSION

Studies of carbon deposition on the anodes of high-temperature fuel cells using internal fuel reforming usually deal with the overall deposition from two main contributions, i.e., the carbon from hydrocarbon dehydrogenation and the carbon monoxide from disproportionation reactions. The system carbon-monoxide-Ni/YSZ anode material was studied with the aim of learning more about its contribution to the overall carbon deposition process and the influence of the anode material on Boudouard's equilibrium.

There are substantial differences in the carbon deposition on the FCM and IAM samples. In dynamic carbon-deposition tests the IAM starts to catalyze the disproportionation of carbon monoxide at lower temperatures and gives a twofold amplitude for this conversion compared to FCM. The IAM sample has a 10 times larger specific surface area than the FCM, and that is probably the reason for its greater activity.

A comparison of the mass of carbon deposited per mg of sample shows that at all four temperatures the amount of carbon deposited is from 1.6 to 3.5 times higher in the case of the IAM sample, with the largest difference between the two samples at the lowest temperature of 400 °C.

The amount of carbon deposited, however, does not represent the only measure of the suitability of materials and conditions that prevail in the anode. The deposition at 700 °C showed that very little carbon was formed and that it, or at least part of it, is reactive enough for the oxidation reaction, while the other part is very stable and does not oxidize up to very high temperatures.

Studies of the carbon deposition on powdered samples of anode materials and their results must be carefully used for the correlation or interpretation of the processes that occur in the anode of a working SOFC. In this study there is no flow of oxygen ions through the electrolyte into the anode and therefore also no electrochemical reactions. Nevertheless, a selective study of

partial reactions and their contribution to the overall deposition can supply valuable data that can be used for designing materials for better and more coke/carbon-resistant anodes.

Acknowledgement

This work was supported by Ministry of Higher Education, Science and Technology and Slovenian Agency of the Republic of Slovenia Grand No. P1-0175: Synthesis, structure, properties of matters and materials and by Sixth European Union Framework Program Biocellus-Biomass Fuel Cell Utility System Contract No. 502759.

5 REFERENCES

- ¹ Eguchi, K., Kojo, H., Takeguchi, T., Kikuchi, R., Sasaki, K.: Fuel flexibility in power generation by solid oxide fuel cells, *Solid State Ionics* 152–153 (2002), 411–416
- ² Huang, T.-J., Wang, C.-H.: Factors in forming CO and CO₂ over a cermet of Ni-gadolinia-doped ceria with relation to direct methane SOFCs, *Journal of Power Sources* 163 (2006), 309–315
- ³ Bartholomew C. H.: Mechanisms of catalyst deactivation, *Applied Catalysis A: General*, 212 (2001), 17–60
- ⁴ Triantafyllopoulos, N. C., Neophytides, S. G.: The nature and binding strength of carbon adspecies formed during the equilibrium dissociative adsorption of CH₄ on Ni-YSZ cermet catalysts, *Journal of Catalysis*, 217 (2003) 324–333
- ⁵ Tu, H., Stimming, U.: Advances, aging mechanisms and lifetime in solid-oxide fuel cells, *Journal of Power Sources*, 127, (2004) 1–2, 284–293
- ⁶ Maček, J., Novosel, B., Marinšek, M. Ni-YSZ SOFC anodes: minimization of carbon deposition. *J. Eur. Ceram. Soc.* [Print ed.], 27 (2007), 487–491
- ⁷ Chen, F., Zha, S., Dong, J., Liu, M.: Pre-reforming of propane for low-temperature SOFCs, *Solid State Ionics* 166 (2004), 269–273
- ⁸ Leng, Y. J., Chan, S. H., Jiang, S. P., Khor, K. A.: Low-temperature SOFC with thin film GDC electrolyte prepared in situ by solid-state reaction, *Solid State Ionics* 170 (2004), 9–15
- ⁹ Takeguchi, T., Kani, Y., Yano, T., Kikuchi, R., Eguchi, K., Tsujimoto, K., Uchida, Y., Ueno, A., Omoshiki, K., Aizawa, M.: Study on steam reforming of CH₄ and C₂ hydrocarbons and carbon deposition on Ni-YSZ cermets, *Journal of Power Sources*, 112 (2002), 588–595
- ¹⁰ Finnerty, C. M., Coe, N. J., Cunningham, R. H., Ormerod, R. M.: Carbon formation on and deactivation of nickel-based/zirconia anodes in solid oxide fuel cells running on methane, *Catalysis Today*, 46 (1998), 137–145